GROUND DATA PROCESSING & PRODUCTION OF THE LEVEL 1 HIGH RESOLUTION MAPS

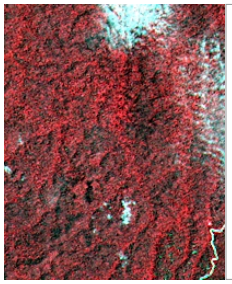

VALERI 2001

Counami site
(tropical forest)

Philippe Rossello

September 2007

CONTENTS

1. Introduction **2**
2. Available data **2**
2.1. SPOT Image 2
2.2. Hemispherical images 3
2.3. Sampling strategy 6
2.3.1. Principles 6
2.3.2. Evaluation based on NDVI values 6
2.3.3. Evaluation based on classification 7
2.3.4. Using convex hulls 9
3. Determination of the transfer function for the 6 biophysical variables: LAIeff, LAItrue, LAI57eff, LAI57true, fCover, fAPAR **10**
3.1. The transfer functions considered 10
3.2. Results 10
4. Conclusion **11**
5. Acknowledgements **11**
ANNEX **12**

1. Introduction

This report describes the production of high resolution, level 1, biophysical variable maps for the Counami site in 2004. Level 1 map corresponds to the map derived from the determination of a transfer function between reflectance values of the SPOT image acquired during (or around) the ground campaign, and biophysical variable measurements (hemispherical images). For each Elementary Sampling Unit (ESU), the hemispherical images were processed using the CAN-EYE software (Version 5) developed at INRA-CSE. The derived biophysical variable maps are:

• four Leaf Area Index (LAI) are considered: effective LAI (LAIeff) and true LAI (LAItrue) derived from the measurement of the gap fraction as a function of the view zenith angle; effective LAI57 (LAI57eff) and true LAI57 (LAI57true) derived from the gap fraction at 57.5°, which is independent on leaf inclination. Effective LAI and effective LAI57 do not take into account clumping effect. LAItrue and LAI57true are derived using the method proposed by Lang and Xiang[1] (1986);

• cover fraction (fCover): it is the percentage of soil covered by vegetation. To improve the spatial sampling, fCover was computed over 0 to 10° zenith angle;

• fAPAR: it is the fraction of Absorbed Photosynthetically Active Radiation (PAR = 400-700nm). fAPAR is defined either instantaneously (for a given solar position) or integrated all over the day. Following a study based on radiative transfer model simulations, it has been shown that the root mean square error between instantaneous fAPAR computed every 30 minutes and the daily fAPAR is the lowest for instantaneous fAPAR at 10h00 AM (solar time, RMSE = 0.021). Therefore, the derivation of fAPAR from CAN-EYE corresponds to the instantaneous black sky fAPAR at 10h00 AM.

The Counami site is covered by the tropical rain forest. It is a large flat plain. The canopy around 20 m high is very dense (see campaign report for more details about the site and the ground measurement campaign: annex or http://www.avignon.inra.fr/valeri).

The site is approximately 4 x 5 km with coordinates described in Table 1:

	UTM 22, North WGS-84 (units = meters)		Geographic Lat/Lon WGS-84 (units = degrees)	
	Easting	Northing	Lat.	Lon.
Upper left corner	249983.7000	594008.6000	5.36985556	-53.25609444
Lower right corner	254023.7000	588968.6000	5.32442873	-53.21949277
Center	252003.7000	591488.6000	5.34714254	-53.23779284

Table 1. Description of the site coordinates.

The ground measurements were carried out from 23rd to 28th September 2001, while the high spatial resolution image (SPOT4, HRVIR1, resolution: 20 m) was acquired in October 2001.

2. Available data

2.1. SPOT Image

The SPOT image was acquired on 18th October 2001 by HRVIR1 on SPOT4. It was geo-located by SPOT image (SPOTView Basic product). The projection is UTM 22, North, WGS-84. No atmospheric correction was applied to the image since no atmospheric data were available. However, as the SPOT image is used to compute empirical relationships between reflectance and biophysical variable, we can assume that the effect of the atmosphere is the same over the whole 4 x 5 km site. Therefore, it will be taken into account everywhere in the same way. Note that the clouds cover 12% of the SPOT image (Figure 1). An unsupervised classification based on the k_means method (ENVI software) was applied to the reflectance of the green and red bands. It allowed to locate the pixels of the cloud cover (Figure 1) and to apply a mask (river in the south-east including).

[1] Lang, A.R.G. and Xiang, Y., 1986. Estimation of leaf area index from transmission of direct sunlight in discontinuous canopies. Agric. For. Meteorol., 37: 229-243.

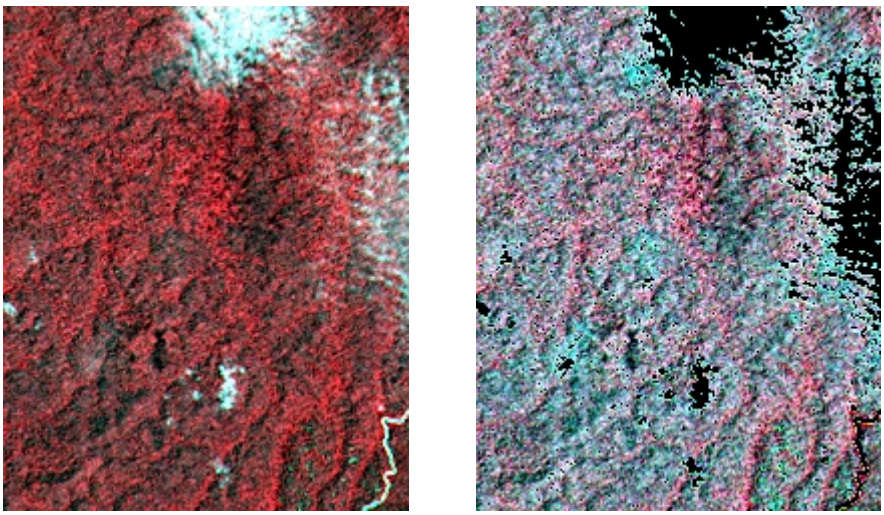

Figure 1. The SPOT image with (left) and without the cloud cover (right). The pixels in black were eliminated (mask).

Figure 2 shows the relationship between Red and near infrared (NIR) SPOT channels: the soil line is marked and no saturated points are observed.

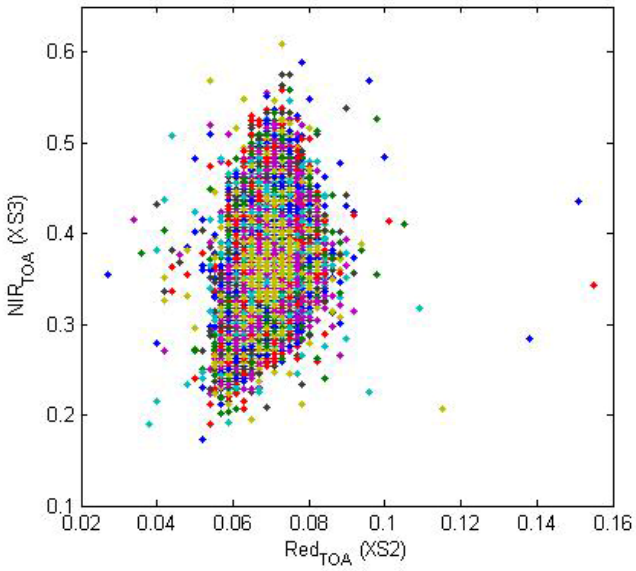

Figure 2. Red/NIR relationship on the SPOT image for Counami, 2001.

2.2. Hemispherical images

The hemispherical images were processed using the CAN-EYE software (Version 5) to derive the biophysical variables. Figure 3 and Figure 4 show the distribution of the several variables over the 48 sampled ESUs. Within the framework of the VALERI project, the hemispherical images are generally acquired from above the understorey and from below the canopy (trees). The two sets of acquisition are processed separately to derive LAI (effective and true), LAI57 (effective and true), fCover, and fAPAR. The ESU biophysical variable was then computed as:

- LAIeff, LAI57eff, LAItrue, LAI57true: LAI(above) + LAI(below).
- fCover: 1-(1-fCover(above))*(1-fCover(below)). This assumes independency between the gaps inside the understorey and those inside the trees which is not true at all the scales but it is the only way to get the total fCover. However, for the local scales considered, this might be true as a first order approximation.
- fAPAR: 1-(1-fAPAR(below))*(1-fAPAR(above)), since 1-fAPAR can be considered equivalent to a gap fraction. Here again, the same independency between the two layers has to be assumed.

For the Counami site, the "canopy is very dense with jointly crowns". As the soil surface is mainly "covered by dead leaves which are quickly decomposed by micro-organisms", the understorey is not taken account. For information, the understorey is only "dense mostly in the thalweg where palm trees are abundant".

Note that LAI (effective and true) derived from directional gap fraction and LAI derived from gap fraction at 57.5° (effective and true) are consistent (Figure 3 and Figure 4). Effective LAI (LAIeff, LAI57eff) varies from 2.7 to 4.33, while true LAI (LAItrue, LAI57true) varies from 3.69 to 7.14. This range shows a homogeneous site in terms of LAI. For values, LAIeff and LAI57eff are lower than LAItrue and LAI57true. This is due to the clumping observed for several ESUs. The relationship between fAPAR and LAI is in agreement with what is expected (Beer-Lambert law) while the fCover-LAI relationship is more noisy (Figure 4). Note that the fCover (except ESU B2bis) and fAPAR values are very high: fCover from 0.71 to 0.91 and fAPAR from 0.92 to 0.98.

To build the relationships between biophysical variables and SPOT data, the reflectance of a given forest ESU was considered as the average reflectance over the central pixel + the 8 surrounding pixels. This takes into account the fact that the height of the trees are about 20 m and consequently the fish-eye observes an area of $\pi \times [20 \times \tan(60°)]^2 = 3770$ m², *i.e.* close to the area of 9 SPOT pixels (= 3600m²) when using a maximum view zenith angle of 60°.

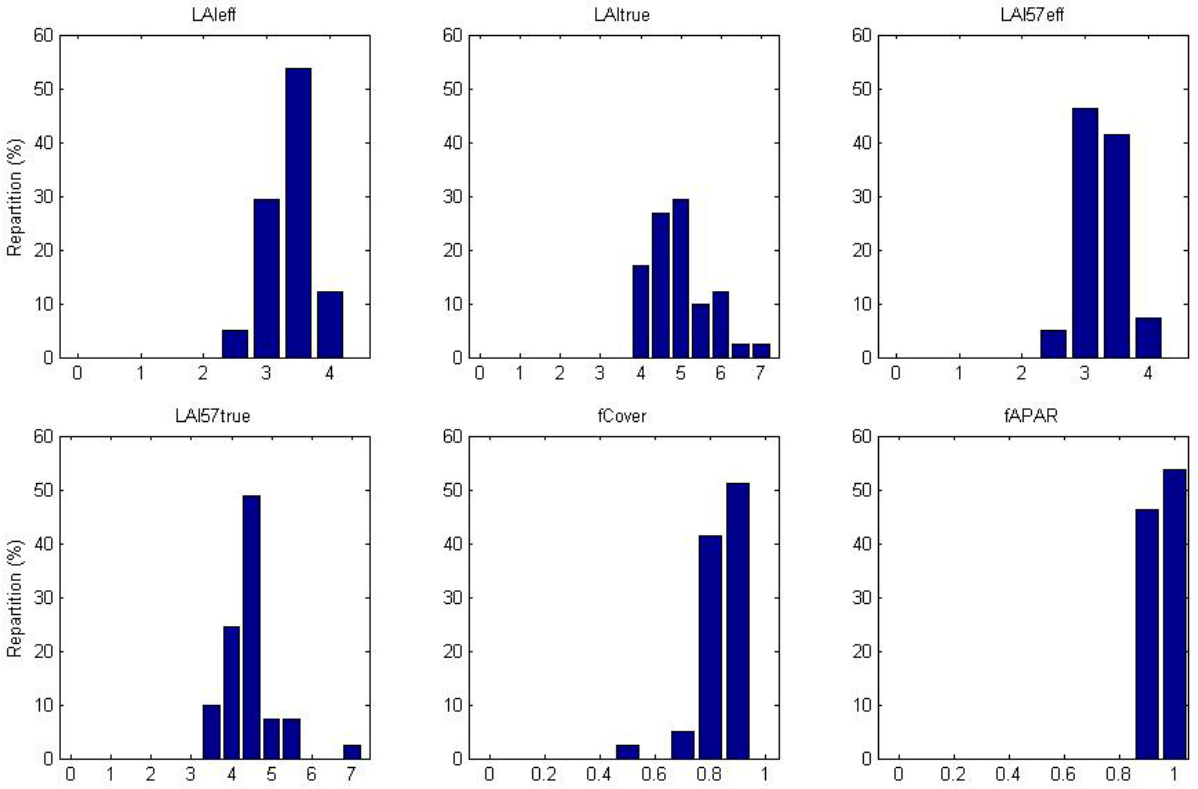

Figure 3. Distribution of the measured biophysical variables over the ESUs.

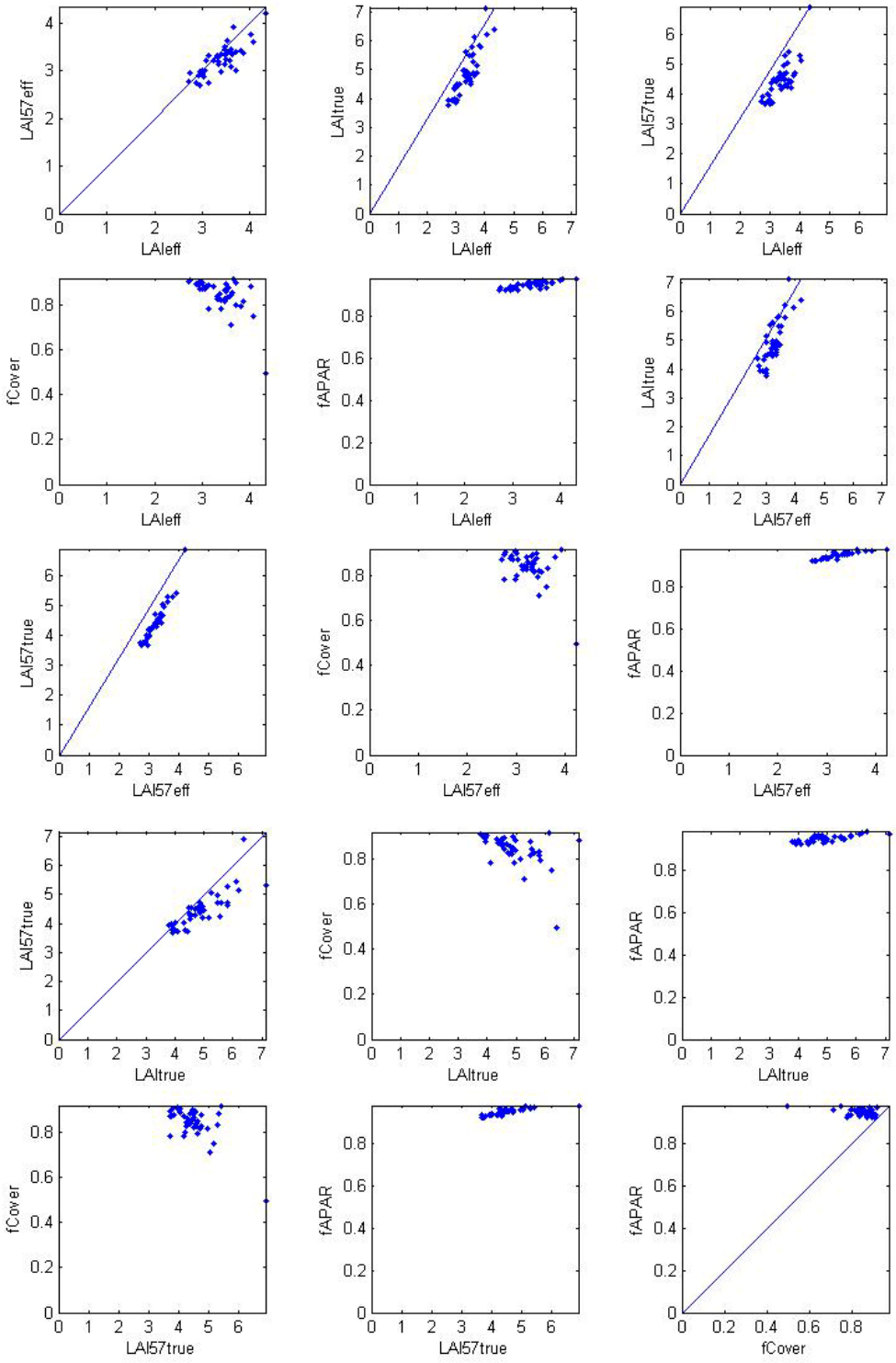

Figure 4. Relationships between the different biophysical variables.

2.3. Sampling strategy

2.3.1. Principles

The sampling strategy is defined in the report on measurement campaign (see campaign report for more details about the site and the ground measurement campaign: annex or http://www.avignon.inra.fr/valeri). The distribution of the ESUs is mainly designed empirically and the sampling of each ESU is based on at least twelve elementary photographs.

Figure 5 shows that the 48 ESUs are evenly distributed over the site (4 x 5 km). The processing of the ground data has shown that B1, C3, F4, I2, J2, K2 and K3 (in black on Figure 5) were located under a cloud. These ESUs were eliminated.

Finally 41 ESUs have been kept for the computation of the transfer function. As the SPOT geo-location and the GPS measurements are not associated to errors, all the ESUs have been kept for the computation of the transfer function.

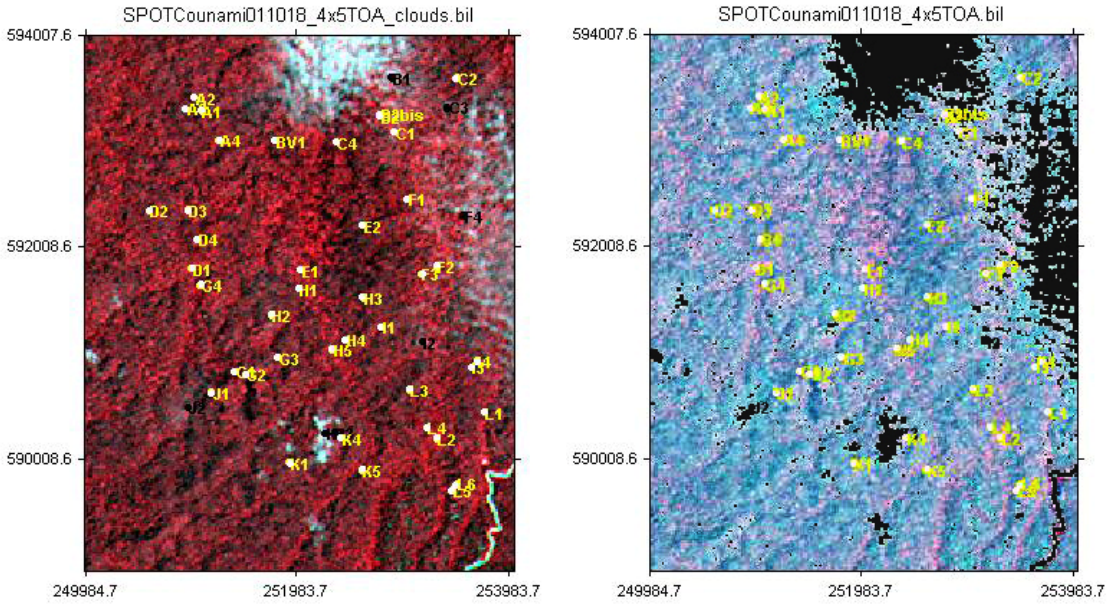

Figure 5. Distribution of the ESUs around the Counami site.

2.3.2. Evaluation based on NDVI values

The sampling strategy is evaluated using the SPOT image by comparing the NDVI distribution over the site with the NDVI distribution over the ESUs (Figure 6). As the number of pixels is drastically different for the ESUs and whole site (WS = 50000 in case of a 4 x 5 km SPOT image, resolution 20 m), it is not statistically consistent to directly compare the two NDVI histograms. Therefore, the proposed technique consists in comparing the NDVI cumulative frequency of the two distributions by a Monte-Carlo procedure which aims at comparing the actual frequency to randomly shifted sampling patterns. It consists in:

1. computing the cumulative frequency of the *N* pixel NDVI that correspond to the exact ESU locations;
2. then, applying a unique random translation to the sampling design (modulo the size of the image);
3. computing the cumulative frequency of NDVI on the randomly shifted sampling design;
4. repeating steps 2 and 3, 199 times with 199 different random translation vectors.

This provides a total population of $N = 199 + 1$(actual) cumulative frequency on which a statistical test at acceptance probability $1 - \alpha = 95\%$ is applied: for a given NDVI level, if the actual ESU density function is between two limits defined by the $N\alpha / 2 = 5$ highest and lowest values of the 200 cumulative frequencies, the hypothesis assuming that WS and ESU NDVI distributions are equivalent is accepted, otherwise it is rejected.

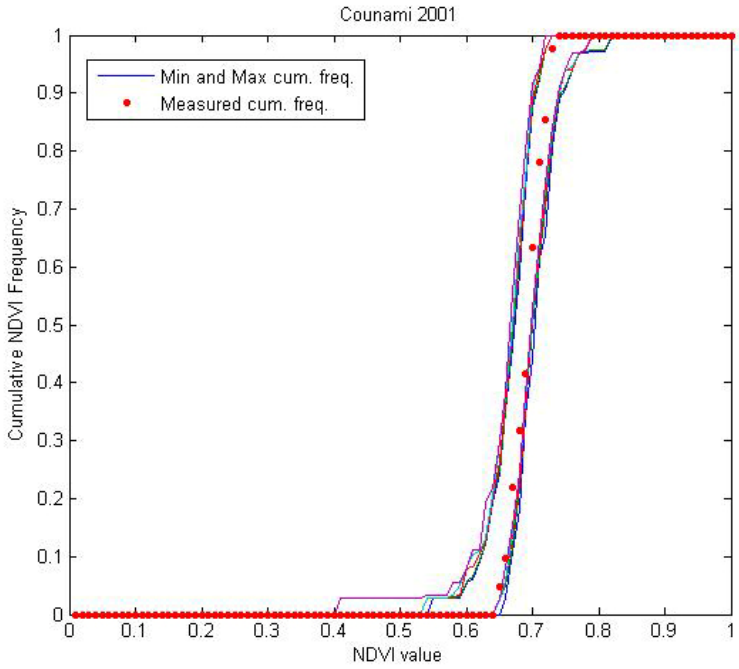

Figure 6. Comparison of the ESU NDVI distribution and the NDVI distribution over the whole image.

Figure 6 shows that the NDVI distribution of the 41 ESUs is very good over the whole site (comprised between the 5 highest and lowest cumulative frequencies), even if the cumulative frequency curve is close to the boundaries (NDVIs < 0.70). Note that NDVI values lower than 0.65 have not been sampled although they are present in the image. The site is homogeneous in terms of NDVI since the highest and lowest distributions are very close.

2.3.3. Evaluation based on classification

A non supervised classification based on the k_means method (Matlab statistics toolbox) was applied to the 4 reflectances of the SPOT image to distinguish if different behaviours on the image for the biophysical variable-reflectance relationship exist.

A number of 5 classes was chosen (Figure 7). Except class 1 (cloud cover), the distribution of the classes on the image and on the ESUs is comparable, even if class 4 is over-sampled.

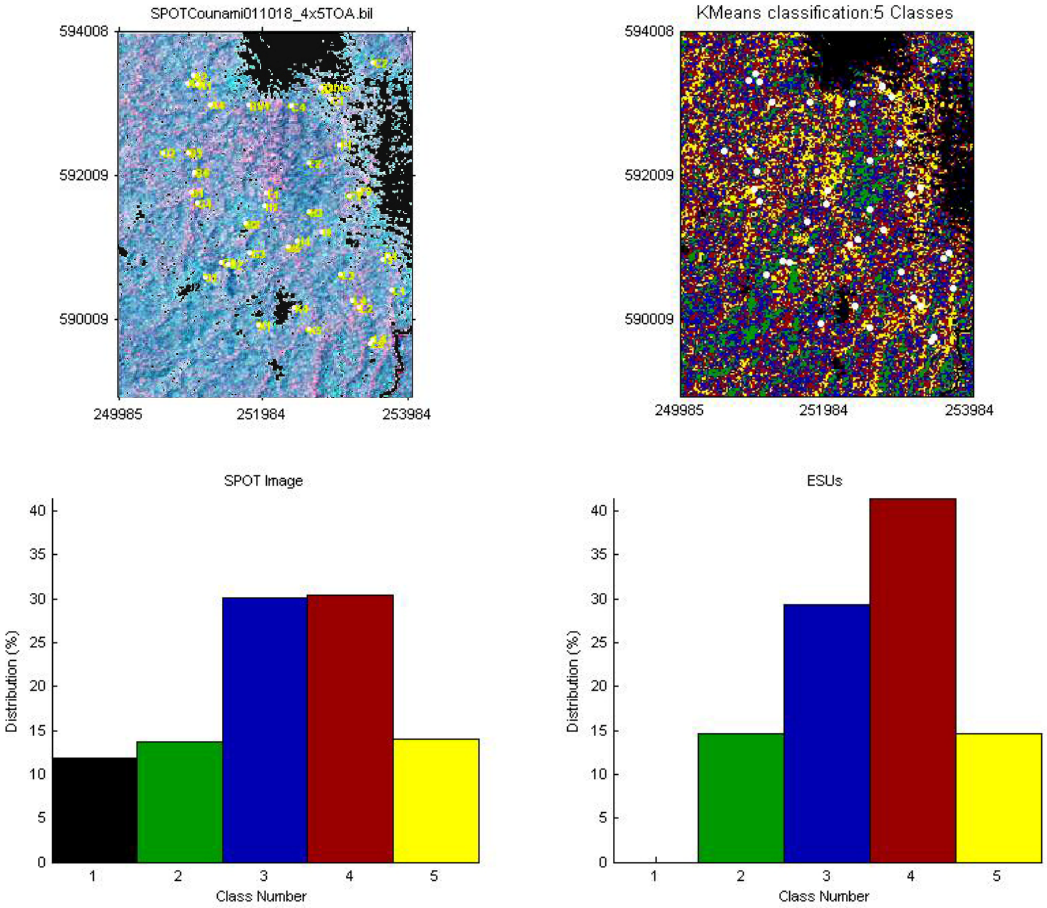

Figure 7. Classification of the SPOT image. Comparison of the class distribution between the SPOT image and sampled ESUs.

Figure 8 shows the different relationships observed between the biophysical variables and the corresponding NDVI on the ESUs, as a function of the SPOT classes determined from non supervised classification.

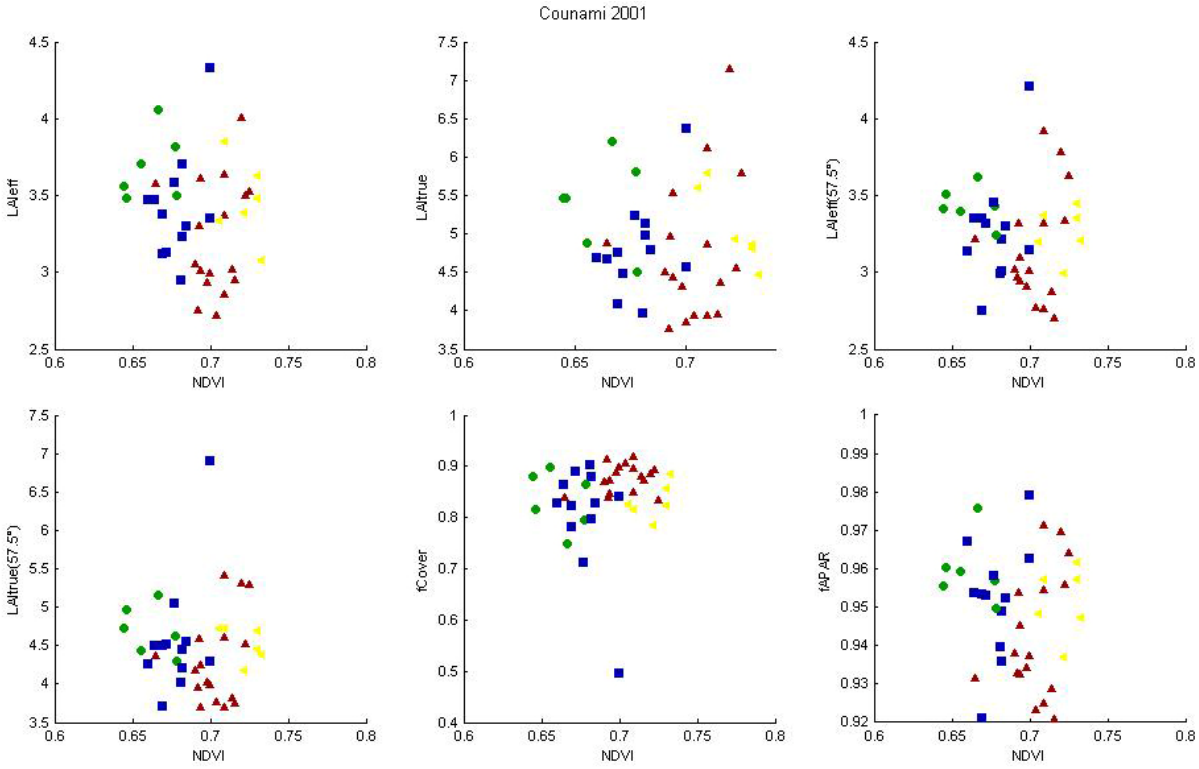

Figure 8. NDVI-Biophysical Variable relationships as a function of SPOT classes

There is no relation between NDVI and biophysical variables due to the fact that the reflectance is saturating for high LAI values. The classes 2, 3, 4 and 5 correspond to the tropical forest. No characteristic behaviour can be observed. Therefore, a single transfer function per variable will be generated. A default value (-0,001) will be attributed to the pixels corresponding to the clouds.

2.3.4. Using convex hulls

A test based on the convex hulls was also carried out to characterize the representativeness of ESUs. Whereas the evaluation based on NDVI values uses two bands (red and NIR), this test uses the four bands of the SPOT image. A flag image, is computing over the reflectances (Figure 9). The result on convex-hulls can be interpreted as:

- pixels inside the 'strict convex-hull': a convex-hull is computed using all the SPOT reflectance corresponding to the ESUs belonging to the class. These pixels are well represented by the ground sampling and therefore, when applying a transfer function the degree of confidence in the results will be quite high, since the transfer function will be used as an interpolator;
- pixels inside the 'large convex-hull': a convex-hull is computed using all the reflectance combination (±5% in relative value) corresponding to the ESUs. For these pixels, the degree of confidence in the obtained results will be quite good, since the transfer function is used as an extrapolator (but not far from interpolator);
- pixels outside the two convex-hulls: this means that for these pixels, the transfer function will behave as an extrapolator which makes the results less reliable. However, having a priori information on the site may help to evaluate the extrapolation capacities of the transfer function.

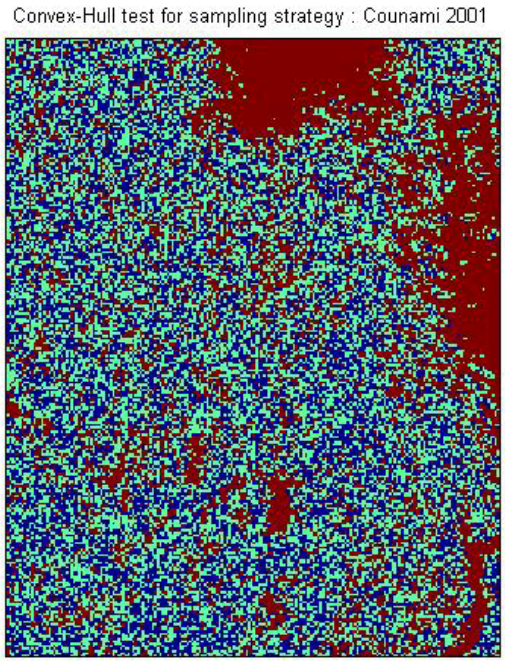

Figure 9. Evaluation of the sampling based on the convex hulls. The map is shown: blue and light blue correspond to the pixels belonging to the 'strict' and 'large' convex hulls and red to the pixels for which the transfer function is extrapolating.

This map shows that the representativeness of the ESUs is good. The pixels outside the two convex-hulls mainly correspond to clouds and river (class 1, §2.3.3).

3. Determination of the transfer function for the 6 biophysical variables: LAIeff, LAItrue, LAI57eff, LAI57true, fCover, fAPAR

3.1. The transfer functions considered

Two types of transfer functions are usually tested in the frame of the VALERI project:

- AVE: if the number of ESUs belonging to the class is too low. The transfer function consists only in attributing the average value of the biophysical variable measured on the class to each pixel of the SPOT image belonging to the class;

- REG: if the number of ESUs is sufficient, multiple robust regression between ESUs reflectance (or Simple Ratio) and the considered biophysical variable can be applied: we used the 'robustfit' function from the matlab statistics toolbox. It uses an iteratively re-weighted least squares algorithm, with the weights at each iteration computed by applying the bisquare function to the residuals from the previous iteration. This algorithm provides lower weight to ESUs that do not fit well. The results are less sensitive to outliers in the data as compared with ordinary least squares regression. At the end of the processing, three errors are computed: classical root mean square error (RMSE), weighted RMSE (using the weights attributed to each ESU) and cross-validation RMSE (leave-one-out method).

As there is no evident relationship between NDVI and LAI (§2.3.3), the results of the multiple robust regression (REG) did not show pertinent results. Therefore, even if the number of ESUs belonging to the classes is sufficient, the 'AVE' method is applied. For each class determined in §2.3.3 (classes 2, 3, 4 and 5), the transfer function consists only in attributing the average value of the biophysical variable measured on the class to each pixel of the SPOT image belonging to the class.

3.2. Results

Following, the results of the transfer function:

	LAIeff	LAItrue	LAI57eff	LAI57true	fCover	fAPAR
Class 1	*-0,001*	*-0,001*	*-0,001*	*-0,001*	*-0,001*	*-0,001*
Class 2	3,688	5,388	3,435	4.700	0,834	0,960
Class 3	3,419	4,819	3,271	4,584	0,805	0,952
Class 4	3,225	4,759	3,152	4,308	0,877	0,942
Class 5	3,462	5,077	3,262	4,528	0,832	0,952

Table 2. Transfer function applied to the whole site for the different biophysical variables

The values of biophysical variable maps are very homogeneous with close values between class 2, 3, 4 and 5. The class 1 values correspond to clouds: a default value (-0.001) is attributed to the pixels belonging to this class. The average value of the ESUs values per biophysical variable over the whole Counami site is also representative:
LAIeff.ESU = 3,3841; LAItrue.ESU = 4,9154; LAI57eff.ESU = 3,2441; LAI57true.ESU = 4,4783;
fCover.ESU = 0,8427; fAPAR.ESU = 0,9491.

4. Conclusion

The transfer function is obtained by using 41 ESUs. The Counami site is homogeneous in terms of LAI and NDVI. However, note that no relationship exists between these two variables. Therefore, the selected transfer function consists in attributing the average value of the biophysical variable measured on the class to each pixel of the SPOT image belonging to the class. Note that a negative value (§2.3.3) is attributed to the pixels belonging to the class 1 (cloud cover). The average value of the ESUs per biophysical variable over the whole site is also representative and consistent with the obtained maps (§3.2).

The Counami site is particular in so far as the estimation of biophysical variables above the tropical forests is difficult. The heterogeneity of the landscape could not be accurately evaluated because of the saturation of the signal due to high LAI values.

The biophysical variable maps are available in UTM, 22 North, projection coordinates (Datum: WGS-84) at 20m resolution.

5. Acknowledgements

We thank **Valéry Gond**, **Onoefé Ngwete**, **Richard Sante** (CIRAD), **Sacha Weber**, **Boris Ruelle** (IRD) and **Frédéric Baret** (INRA) who participated to the field experiment, but also **Benjamin Baret** (INRA) who processed the hemispherical images**.**

ANNEX

VALERI – 2001 Field campaign in Counami (French Guiana)

Participants:

BARET Frédéric (INRA)
GOND Valéry (CIRAD)
NGWETE Onoefé (CIRAD)
RUELLE Boris (IRD)
SANTE Richard (CIRAD)
WEBER Sacha (IRD)
September 23-28, 2001

The VALERI-2001 field campaign carried out in the tropical rain forest in French Guiana, took place in the middle of the dry season (July-November). This period is optimal to acquire simultaneously high resolution SPOT images and field data. This is also the only period where the forest is accessible in reasonable conditions. The main goal was to measure leaf area index to describe the spatial heterogeneity of this complex ecosystem. The mission was possible with the co-ordination of three institutions (CIRAD, INRA and IRD). The choice of the Counami forest was driven by its accessibility by a stone-way and the possibility to lodge there in a hut for several days during the experimentation. Counami forest is also a study area for ecologists from different institutions in French Guiana.

Site description

The Counami forest is located in the Northern part of the Amazon forest on the North-Eastern slope of the Guiana's plateau in French Guiana (Figure 1). The geographic location is 5°21' North and 53°15' East. Situated 50 km away from the Ocean, the landscape is an evergreen tropical forest with 2750 mm of rainfall per year and a mean annual temperature of 26°C. Diurnal variations do not exceeds 12°C and the hygrometry is between 80% during dry season and 90% during rainy season.

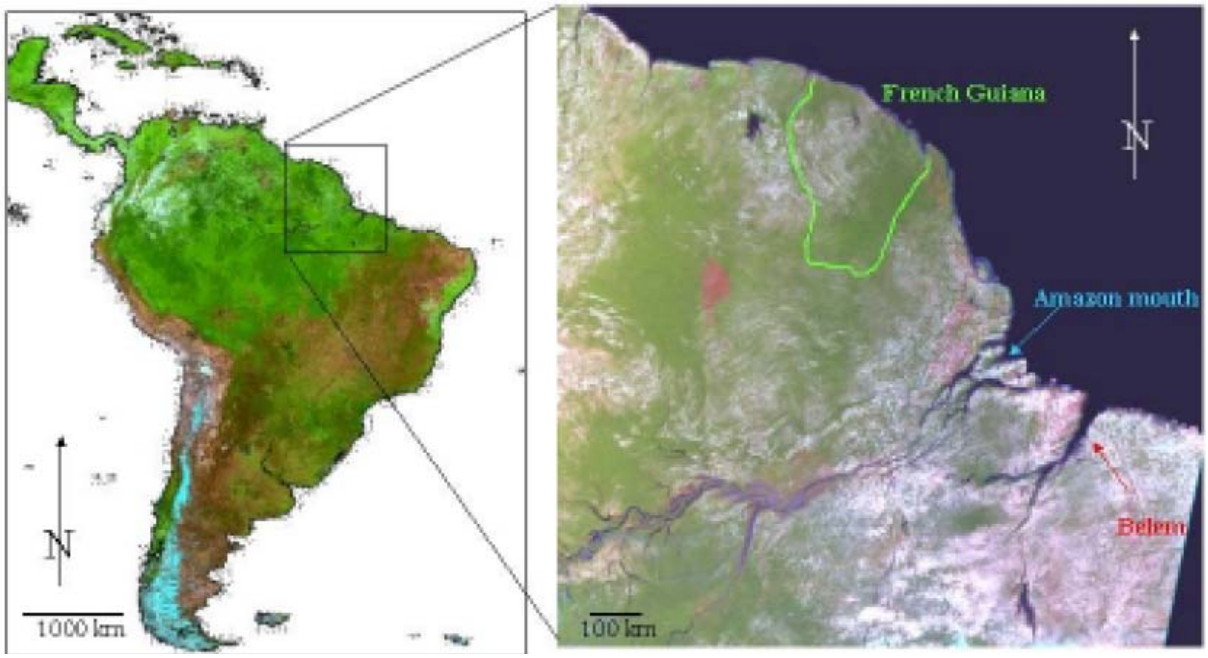

***Figure 1**: Geographic context of South America on the left (SPOT-4 VEGETATION S10 data). On the right a zoom over the Northern Amazon basin with French Guiana (in green) (SPOT-4 VEGETATION S1 data).*

Counami's landscape is a large flat plain resulting from a long period of erosion. The geology is mainly an old shale substratum (2.1 billion year) with granite intrusions. Geomorphology of the area is a consequence of the permanence of the warm and wet climate which induces a chemical weathering named ferralitization. Kaolinitic clay is the result of this weathering and can be very thick from 10 to 70m deep. The aspect of the landscape in these areas is a large plain covered by hemispheric hills (20 to 50m high) separated by a dense drainage network. It is the well known half-orange relief of the tropical regions. At the top of some hills it is possible to have iron-pans or gravels resulting from dryer paleo-climates which influence locally the soil distribution. In these conditions different soils were developed depending on the slope and the altitude (Freycon, 2001). Considering the FAO-

Unesco soils classification the soils present in Counami forest are classified as ferralsols (Driessen & Dudal, 1991). Water percolation in these soils is the main factor of the forest structure distribution (Sabatier, et al. 1997). From the top to the bottom of the hill, the impervious clay horizon goes closer to the soil surface and block water percolation and roots development (Paget, 1999; Clark & Clark, 2000). So, the structure of the forest depends on the topographic situation (plateau, slope or thalweg).

Characteristic of the tropical rain forest, the study site is composed by many different tree species, barely 150/ha (Nelson, et al. 1990 ; Whittaker, et al. 2001) . This richness is due to the low extinction rate due to the absence of glaciation and a high level of species diversity due to the alternation of dry and wet periods during the Quaternary (Molino & Sabatier, 2001). The main canopy is around 30m high with emergent trees at 40m high. The canopy is in general very dense with jointly crowns. Most of the trees have a diameter between 10 to 60cm. Some of them have a diameter of 1 or 2m (in general on the plateau). The paradox is that this forest is homogeneous in its heterogeneity. The understory is generally dense mostly in the thalweg where palm trees are abundant. A lot of lianas and epiphytes climb on the tall trees. The soil surface is covered by dead leaves (layer of 5 to 10 cm) which are quickly decomposed by micro-organisms. Seen from above the forest appears very compact. As shown with an aerial photography, it is difficult to identify differences between the forest types (Figure 2). The relief appears strongly with shades and sun faces but a delimitation between forest types is difficult, even for a photo-interpreter (Trichon, 2001). Several techniques try to resolve, at this scale, the ambiguities to determine stand structure in these non-perturbed by human activities forests.

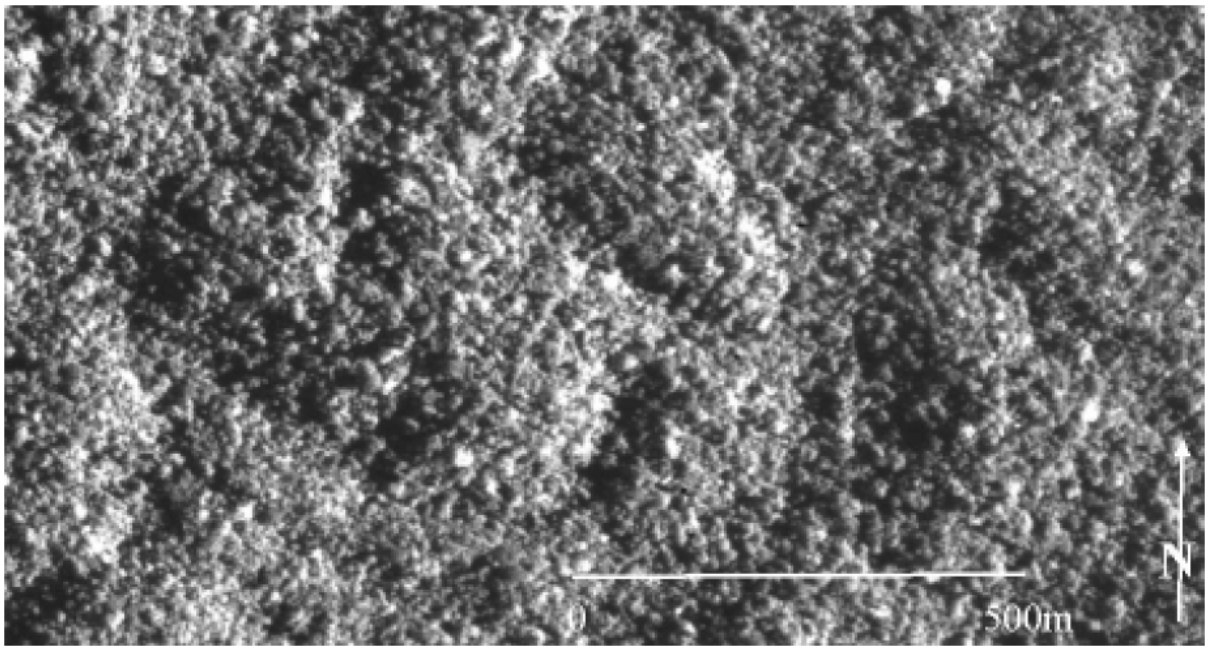

***Figure 2**: An aerial photography of the Counami forest (1981). The half-orange relief is covered by the tropical rain forest.*

Material used

All measurements were made by two separated teams, from September 24 to September 27 between 10:00 (a.m.) and 17:00 (p.m.). The LAI measurements were made with two Nikon Coolpix 990 digital cameras using fish-eye lenses (360°). The cameras were installed on a 60cm high tripod to avoid perturbation from the user and to keep a standard position (50 cm above the ground level) of the sensors during the experiment. This was possible because of the scarcity of vegetation below 60cm.

The geographical position of the measurement sites was pre-established using a 1/50.000° topographic map. During the field measurements two GPS instruments (Garmin CX12 and Magellan C815) were used to catch geographic position in a WGS84 ellipsoïd reference. A minimum of three satellites were used to get a maximum precision in the measures under the canopy. Otherwise an approximate position was written down on the topographic map. An integrated photosynthetic active radiation (400 – 700 nm) sensor (BF2 instrument) was installed 30km East of the Counami forest, in a safer area for autonomous measurements (Paracou, 5°16'North – 52°57'West). This instrument was used to measure direct and diffuse sun radiation from September 18, to October 16. Installed in a flat position the instrument was supplied with a 12V battery.

A simultaneous remote sensing acquisition was planned with the SPOT-Images company (KJ 689-339). From September 1 to November 1, four quick-looks were delivered (September 7, September 12, October 18 and October 19). Because no clouds were identified over the study area for October 18 (day 291), this scene was acquired. Calibration and navigation were processed by the SPOT-Images company in Toulouse. According to landmark measurements using GPS in November 2001, the geo-location of the SPOT data was also processed in the referenced system WGS84.

A field-card was established to note quickly during the measurements different information about the environment of the measurement sites. These field-cards are numbered and described the situation (location, type, slope, exposition, hydrology), soil (aspect, structure), canopy and understory (diameter, height, liana, damages).

Method employed

The method employed during this study was driven by the idea of taking into account the spatial heterogeneity in the continuum of the forest canopy. The spatial integration of LAI measurements related with remote sensing data, developed in the VALERI program, was a permanent preoccupation.

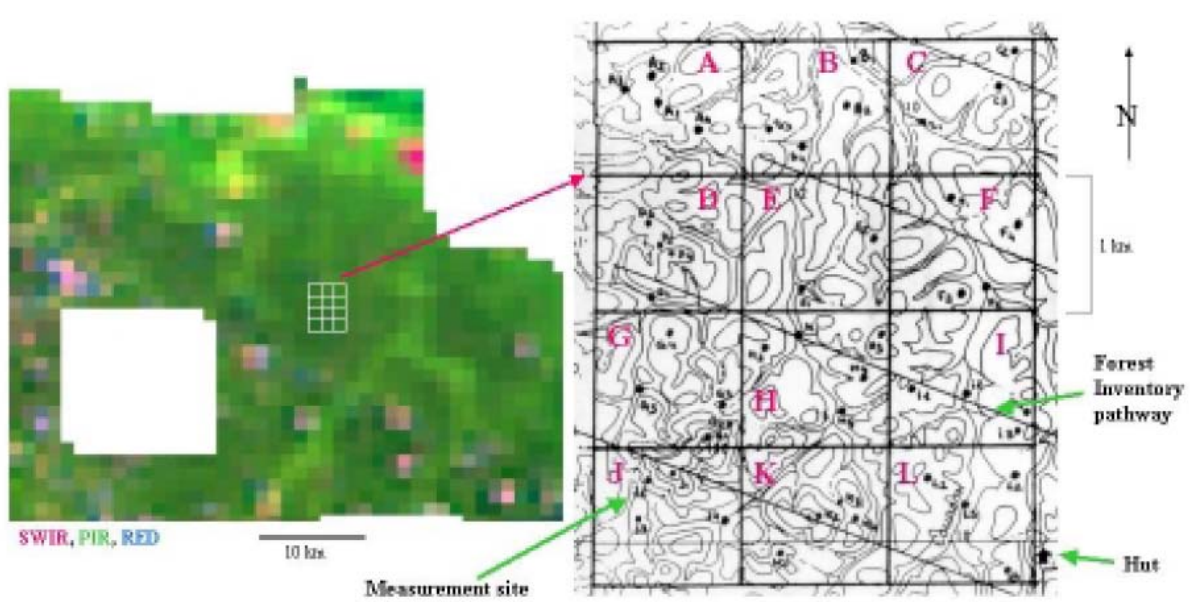

***Figure 3**: Measurement sites in the 12 different SPOT-4/VEGETATION pixels. Each measurement was pre-located and definitely chosen in the field depending on the access. Each point was geo-located by GPS.*

According to the location of SPOT-4 / VEGETATION data, 12 pixels were delimited on the topographic map (Figure 3). Each pixel was named from A (upper-right corner) to L (bottomleft corner). In each pixel a set of four measurement sites was selected representing four distinct environments identified from the topographic map as (i) thalweg along the waterways, (ii) plateau with their large top tables, (iii) gentle slope (<20%) and (iv) steep slope (>20%). Each of these four environments are characterised by different forest structures. As seen on Figure 3 the pixels were superimposed to a network of forest inventory pathways. This network allows the access to the different parts of the forest. During the field measurements the locations of the chosen sites were adapted to the accessibility. For each point a geographic position was systematically established (GPS). Then a group of 12 measurements, to be consistent with the VALERI protocol, was made using the fish-eye digital camera. This group is oriented to the North within a square of 20m side. Nine measurements were completed with three randomly distributed measurements inside the square (Figure 4).

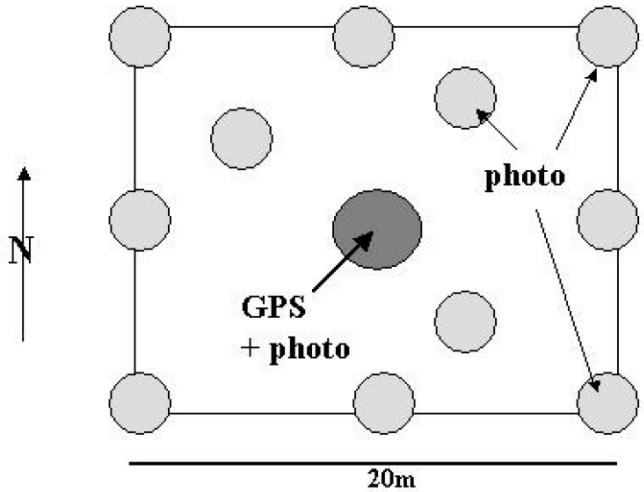

***Figure 4**: Fish-eye measurements protocol for each site. Height measurements were made on the sides of a 20m square located around the central point of the measurement site as well as one at this central point. Three randomly choose measurements were also made. All the measurements were oriented with a compass and geo located by GPS.*

Results

Fish-eye measurements were carried out on 44 measurement sites representing 528 hemispherical pictures (Figure 5). The two teams made measurements on the same site in order to establish a "calibration point". Two sets of twenty simultaneous measurements were made along a line starting in a natural area through a deforested area and ending in a natural area again, in order to observe LAI variations linked with human activities. At the end 592 hemispherical pictures were collected.

***Figure 5**: Thalweg fish-eye picture in the tropical forest of Counami. Observe Palm tree in the understory and the density of the cover.*

Discussion and perspectives

The field campaign was satisfactory because of the good spatial sampling and the amount of data collected. Concerning the Nikon Coolpix 990C, only a battery problem perturbed the measurement in pixel E (only 2 measurement site). A problem also happened in pixel B where the two teams worked simultaneously, and a large part of the pixel's centre was not documented. The use of hemispherical cameras was very convenient because of their weights and easy manipulation. This experiment could not have been accomplished with instruments like LAI-2000 for example. In general the weather was good except several rain showers in the afternoon which disturbed the measurements due to rain drops on the lenses.

About the GPS it could be said that the location was sometimes difficult to obtain due to the density of the vegetation. Three satellites signals were the minimum to get an acceptable precision in the position. The rain has strongly disturbed the GPS measurements. When GPS locations were transferred on the topographic map, a shift in the position was noted. This is due to the different ellipsoids used in these different systems. GPS used the WGS84 and topographic map Clark1880. The shift noted was from 30 to 100m to the North for GPS location taking the topographic map as a reference. The position transfer on the topographic

map was possible with the information noted on the field-cards. It was observed that the Garmin CX12 seems to shift less than the Magellan C815.

The BF2 had several problems with the data logger. This failure was probably due to an electric supplies problem. At the end the data were lost because of a bad manipulation of the battery. No data are available in sun radiation.

The SPOT-HRV image was acquired very late (one month after the field measurements).

References

Clark, D.B. & Clark, D.A., 2000, Landscape-scale variation in forest structure and biomass in a tropical rain forest, *Forest Ecology and Management*, **137**: 185-198.

Driessen, P. M. and Dudal, R., 1991, The major soils of the world, Agricultural University Wageningen, The Netherlands, 310 pages (ISBN 90-800725-1-6).

Freycon, V., 2001, Etude comparative des systèmes sols sur deux unités de paysage du massif de Counami (Guyane française). Note CIRAD-Forêt, Kourou, 32 pages.

Molino, J-F. and Sabatier, D., 2001, Tree diversity in tropical rain forests: a validation of the intermediate disturbance hypothesis. *Science*, In press.

Nelson, B., Ferriera, C. A. C., Da Silva, M. F. and Kawasaki, M. L., 1990, Endemism centres, refugia and botanical collection density in Brazilian Amazon. *Nature*, **345**: 714-716.

Paget, D., 1999, Etude de la diversité spatiale des écosystèmes forestiers guyanais : réflexion méthodologique et application. *Thèse de Doctorat*, ENGREF, Paris, 154 pages.

Sabatier, D., Grimaldi, M., Prévot, M-F., Guillaume, J., Godron, M., Dosso, M. and Curmi, P., 1997, The influence of soil cover organization on the floristic and structural heterogeneity of a Guianan rain forest. *Plant Ecology*, **131**: 81-108.

Trichon, V., 2001, Crown typology and the identification of rain forest trees on large-scale aerial photographs, *Plant Ecology*, **153**: 301-312.

Whittaker, R. J., Willis, K. J. and Field, R., 2001, Scale and species richness: towards a general, hierarchical theory of species diversity. *Journal of Biogeography*, **28**: 453-470.